

# Functional Expression of Multidrug Resistance Protein 1 in *Pichia pastoris*<sup>†</sup>

Jie Cai,<sup>‡</sup> Roni Daoud,<sup>§</sup> Elias Georges,<sup>§</sup> and Philippe Gros<sup>\*,‡</sup>

Department of Biochemistry and Institute of Parasitology, McGill University, Montreal, Quebec, Canada H3G 1Y6

Received January 16, 2001; Revised Manuscript Received April 24, 2001

**ABSTRACT:** Overexpression of the multidrug resistance-associated protein (MRP1) causes multidrug resistance in cultured cells. MRP1 transports a large number of glutathione, glucuronide, and sulfate-conjugated organic anions by an ATP-dependent efflux mechanism. Six other MRP proteins exist (MRP2–7), and mutations in some of these genes cause major pathological conditions in humans. A detailed characterization of the structure and mechanism of action of these proteins requires an efficient expression system from which large amounts of active protein can be obtained. We report the expression of a recombinant MRP1 in the methylotrophic yeast *Pichia pastoris*. The protein is expressed in the membrane fraction of these cells, as a stable and underglycosylated 165 kDa peptide. Expression levels are very high, and 30 times superior to those seen in multidrug-resistant HeLa/MRP1 transfectants. MRP1 expressed in *P. pastoris* binds 8-azido[ $\alpha$ -<sup>32</sup>P]ATP in a Mg<sup>2+</sup>-dependent and EDTA-sensitive fashion, which can be competed by a molar excess of ADP and ATP. Under hydrolysis conditions (at 37 °C), orthovanadate induces trapping of the 8-azido[ $\alpha$ -<sup>32</sup>P]nucleotide in MRP1, which can be further modulated by known MRP1 ligands. MRP1 is also labeled by a photoactive analogue of rhodamine 123 (IAARh123) in *P. pastoris*/MRP1 membranes, and this can be competed by known MRP1 ligands. Finally, MRP1-positive membrane vesicles show ATP-dependent uptake of LTC<sub>4</sub>. Thus, MRP1 expressed in *P. pastoris* is active and shows characteristics of MRP1 expressed in mammalian cells, including drug binding, ligand-modulated formation of the MRP1–MgADP–P<sub>i</sub> intermediate (ATPase activity), and ATP-dependent substrate transport. The successful expression of catalytically active and transport-competent MRP1 in *P. pastoris* should greatly facilitate the efficient production and isolation of the wild type or inactive mutants of MRP1, or of other MRP proteins for structural and functional characterization.

The emergence of multidrug resistance in cultured cells in vitro and tumor cells in vivo has been associated with the overexpression of two members of the ABC family of transporters, P-glycoprotein (P-gp)<sup>1</sup> and multidrug resistance-associated protein 1 (MRP1) (1, 2). Transport studies have shown that these transporters function as drug efflux pumps to reduce intracellular accumulation of a large group of

structurally unrelated drugs (3–5). Within the ABC family, MRP1 belongs to a subgroup of structurally and functionally distinct proteins that includes, among others, the yeast cadmium resistance factor YCF1 (6, 7), the oligomycin resistance protein YORI (8), the bile acid transporter BAT1 (9), and the mammalian sulfonyleurea receptors SUR1 and SUR2 (10, 11). This group of ABC transporters is characterized by the presence of a unique N-terminal membrane-associated domain possibly encoding 5 TM segments, in addition to the 12-TM domain, 2-NBD structure characteristic of many ABC transporters (12, 13). Although P-gp can act on unmodified drugs, transport studies in MRP1-positive cells and in membrane vesicles derived from them have established that MRP1 functions as a GS-X pump and transports drugs conjugated to glutathione (GSH), glucuronide, or sulfate, and may transport unmodified drugs together with GSH (2, 14, 17). Known substrates of MRP1 include etoposide (VP16) and steroid glucuronides, cysteinyl leukotrienes, dinitrophenylglutathione, and bile salt derivatives (5, 15–18). A possible role of MRP1 in resistance to cancer chemotherapy in vivo has been suggested by RNA expression studies in primary tumors (19).

MRP1 is not a single gene, but is part of a gene family that includes at least six or seven members in humans (MRP1–7) whose amino acid sequences are between 33 and 58% identical. While MRP2, MRP3, and MRP6 have predicted secondary structures similar to that of MRP1,

<sup>†</sup> This work was supported by research grants to P.G. from the National Cancer Institute of Canada and to E.G. from the Natural Sciences and Engineering Research Council of Canada. P.G. is an International Research Scholar of the Howard Hughes Medical Institute and a Distinguished Scientist of the Canadian Institutes of Health Research.

\* To whom all correspondence should be addressed: Department of Biochemistry, McGill University, 3655 Sir William Osler Promenade, Room 907, Montreal, PQ, Canada H3G 1Y6. Phone: (514) 398-7291. Fax: (514) 398-2603. E-mail: gros@med.mcgill.ca.

<sup>‡</sup> Department of Biochemistry.

<sup>§</sup> Institute of Parasitology.

<sup>1</sup> Abbreviations: ABC, ATP binding cassette; AOX, alcohol oxidase; BSA, bovine serum albumin; DOX, doxorubicin; EDTA, ethylenediaminetetraacetic acid; EGTA, ethylene glycol bis( $\beta$ -aminoethyl ether); HA, hemagglutinin A; IAARh123, iodoaryl azidorhodamine 123; LTC<sub>4</sub>, leukotriene C<sub>4</sub>; LTD<sub>4</sub>, leukotriene D<sub>4</sub>; Mg<sup>2+</sup>, magnesium ion; MRP, multidrug resistance-associated protein; Mut<sup>s</sup>, methanol-utilizing slow; MVs, membrane vesicles; NBD, nucleotide binding domain; PCR, polymerase chain reaction; P-gp, P-glycoprotein; P<sub>i</sub>, phosphate; PNGase F, peptide N-glycosylase F; Rh123, rhodamine 123; SDS–PAGE, sodium dodecyl sulfate–polyacrylamide gel electrophoresis; TM, transmembrane; TXL, paclitaxel or Taxol; UTR, untranslated region; UV, ultraviolet; VBL, vinblastine; VCR, vincristine; V<sub>i</sub>, (ortho)vanadate; VP16, etoposide.

MRP4 and MRP5 are predicted to lack the additional N-terminal membrane-associated domains characteristic of MRP1 (20–23). Biochemical and genetic studies have established that MRP family members play key physiological roles and that mutations in these genes cause significant clinical pathologies. Indeed, MRP2, also known as the canalicular multispecific organic anion transporter (cMOAT), is expressed at the canalicular membrane of hepatocytes, where it transports a wide range of anionic conjugates into the canalicular space (24–26). Mutations in *MRP2/cMOAT* cause Dubin-Johnson syndrome (DJS) in humans (27–29), and an increased level of expression of *MRP2/cMOAT* in transfected cells is associated with increased resistance to drugs such as vinblastine (VBL), cisplatin (CDDP), adriamycin (ADR), and VP16 (30, 31). On the other hand, MRP3 transports glucuronide conjugates and methotrexate (32). Transfection studies show that MRP3 overexpression causes low-level resistance to VP16 and teniposide (33), and gene expression studies in lung carcinoma cell lines have shown a relationship between *MRP3* mRNA expression and resistance to natural product drugs and CDDP (34). Finally, mutations in the *MRP6* gene are associated with pseudoxanthoma elasticum (PXE) in humans, a heritable disorder of the connective tissue associated with skin lesions, visual field loss, and defects in the cardiovascular system (35, 36). Therefore, a better understanding of the mechanism of action of MRP1 and other MRP proteins in normal tissues would be important for successful intervention in the corresponding diseases, including drug-resistant tumors.

As they have for P-gp, photolabeling studies have shown that MRP1 can directly interact with drug substrates, and that TM domains play a key role in such interactions. Indeed, MRP1 can be photolabeled by analogues of leukotriene C<sub>4</sub> (LTC<sub>4</sub>) (15), as well as by photoactive analogues of a quinoline (IACI) (37) and rhodamine (IAARh123) (38). Studies with the latter two compounds have identified photolabeling sites in the second and third large membrane-associated portions of the protein. Studies in MRP1-positive intact cells and membrane vesicles have clearly established that MRP1-mediated transport is ATP-dependent (39). In membrane fractions, MRP1 can be photolabeled with 8-azido- $[\alpha\text{-}^{32}\text{P}]\text{ATP}$  in the presence of magnesium ( $\text{Mg}^{2+}$ ) and orthovanadate ( $\text{V}_i$ ) (40). Vanadate-induced nucleotide trapping in MRP1 can be stimulated by anticancer drugs and by glutathione (40), a first indication that MRP1 may possess substrate-stimulated ATPase activity. Studies with MRP1 purified and reconstituted in liposomes have confirmed that MRP1 has intrinsic ATPase activity, which is vanadate-sensitive, and can be further stimulated by drug substrates, glutathione, and LTC<sub>4</sub> (41, 42), although large differences in  $K_m$  and  $V_{\text{max}}$  were reported in these studies. Both NBD1 and NBD2 are required for ATP hydrolysis by MRP1, as mutations in the Walker A and B motifs in either site drastically reduced the level of ATP hydrolysis and transport by the protein (43, 44). Moreover, MRP1 ATPase activity can be significantly stimulated by certain nucleotide diphosphates (45). Additional photolabeling studies of the wild type, mutant variants, and half-molecules of MRP1 with 8-azido- $[\alpha\text{-}^{32}\text{P}]\text{ATP}$  or 8-azido- $[\gamma\text{-}^{32}\text{P}]\text{ATP}$  strongly suggest that the two NBDs are not functionally equivalent in MRP1 but may allosterically interact. Indeed, it appears that MRP1 exclusively binds to 8-azido- $[\alpha\text{-}^{32}\text{P}]\text{ATP}$  at NBD1 while hydrolysis

preferentially takes place at NBD2 (43, 44, 46). In addition, Hou et al. have proposed a catalytic model for MRP1, which is based on alternate site catalysis but also includes a phosphorylated intermediate of the protein (44).

The biochemical basis of MRP1 transport, including the ATPase activity of the protein and its regulation by substrates and inhibitors, is best studied in purified preparations of the protein. In addition, structural information about the protein gained by infrared spectroscopy, or by fluorescence of endogenous tryptophans and/or modified cysteine residues, also requires highly pure protein preparations. So far, MRP1 has been purified (MRP1-His<sub>10</sub>) from detergent extracts of transfected baby hamster kidney (BHK) cells by affinity chromatography on  $\text{Ni}^{2+}$ -chelate columns (41). Alternatively, a purification procedure from plasma membranes of highly MRP1-expressing H69AR cells, based on differential CHAPS extraction and immunoaffinity purification using the anti-MRP1 monoclonal antibody QCRL-1, has been described (42). Although these methods are suitable for the preparation of small amounts of active protein, they are both expensive and time-consuming and do not allow the study and purification of inactive mutants generated by site-directed mutagenesis. *Pichia pastoris* is a methylotrophic yeast that can use methanol as a sole source of carbon for growth. For this, it relies on the strong induction of alcohol oxidase 1 (AOX1) (47, 48), a characteristic used to develop a highly efficient system for recombinant protein expression. In this system, heterologous cDNAs are introduced at the endogenous *AOX1* locus by homologous recombination, followed by induction of the cloned cDNA expression by culturing the cells in methanol-containing medium. Our laboratory has previously reported the expression and purification of large amounts of catalytically active and highly pure mouse Mdr3 P-gp from *P. pastoris* (49, 50). In the study presented here, we report high-level expression and functional characterization of MRP1 in *P. pastoris*.

## MATERIALS AND METHODS

**Materials.** The *P. pastoris* expression system, including the plasmid expression vector pHIL-D2, and tester strains GS115 and KM71 were purchased from Invitrogen (License 145457). The pJ3 $\Omega$ -MRP1 plasmid containing the full-length MRP1 cDNA was a generous gift of P. Borst (The Netherlands Cancer Institute, Amsterdam, The Netherlands). Mouse monoclonal anti-hemagglutinin A (HA) antibody 16B12 was purchased from Babco Labs (Richmond, CA). The MRP1 specific mouse monoclonal antibody QCRL-1 was purchased from ID Laboratories (London, ON). Oligonucleotides used for constructing the recombinant MRP1 cDNA were ordered from Gibco BRL (Montreal, PQ). 8-Azido- $[\alpha\text{-}^{32}\text{P}]\text{ATP}$  (specific activity of 10–20 Ci/mmol) was purchased from ICN.  $[\text{I}^{25}]\text{IAARh123}$  was prepared as previously described (38). Protein A-Sepharose was purchased from Pharmacia Inc. (Montreal, PQ). The leukotriene D<sub>4</sub> (LTD<sub>4</sub>) receptor antagonist MK571 was kindly provided by A. W. Ford-Hutchinson (Merck-Frost Centre for Therapeutic Research, Quebec City, PQ). LTC<sub>4</sub> was purchased from Cayman Chemical Co. (Ann Arbor, MI).  $[\text{I}^{14}, \text{I}^{15}, \text{I}^{19}, \text{I}^{20}\text{-}^3\text{H}]\text{LTC}_4$  (146 Ci/mmol) was purchased from DuPont NEN (Mississauga, ON). All other chemicals were of the highest commercial grade available.

**MRP1 cDNA Cloning.** The full-length cDNA for MRP1 from plasmid pJ3 $\Omega$ -MRP1 (51) was modified in the 5' and

3'-untranslated (UTR) sequences to enhance expression of the protein in yeast. First, the 5'-UTR was altered by PCR mutagenesis to reduce its length and to introduce a *Sac*II site followed by six adenosines just upstream of the ATG initiation codon (underlined) of the *MRP1* cDNA. For this, oligonucleotides JC-4 (5'-AGGCCGCGGAAAAAATG-GCGCTCCGGGGCTTC-3') and JC-10 (5'-GACGATCAAA-GCCTCCACC-3', complementary to the *MRP1* encoding nucleotide positions 751–868) were used. The PCR product was gel purified and cleaved with *Sac*II and *Bam*HI, and the 750 bp fragment was then reintroduced into the full-length *MRP1* cDNA. The 3'-end was modified by addition of a *Sna*BI linker immediately upstream of the stop codon, using mutagenic oligos JC-1 (5'-CCGGCTTGGTGTAC-3') and JC-2 (5'-GTACACCAAG-3'), which contain a cohesive *Ngo*MI end at the 5'-terminus and a blunt *Sna*BI half-site at the 3'-end. The oligos were annealed and ligated to a 4.5 kb *Sac*II–*Ngo*MI restriction fragment to form the full-length *MRP1* cDNA. The pHIL-D2 vector was previously modified to contain a *Sac*II site (for the 5'-end) and a *Sna*BI site (for the 3'-end), followed by a hexahistidine tag (52) (I. L. Urbatsch et al., unpublished observations). The modified full-length *MRP1* cDNA, isolated as a *Sac*II–*Sna*BI fragment, was then cloned into the *Sac*II and *Sna*BI sites of the modified *P. pastoris* expression plasmid pHIL-D2, resulting in the recombinant plasmid pHIL-MRP1-His<sub>6</sub>. Finally, an antigenic HA epitope tag (sequence YPYDVPDYAS) was then inserted at the *Sna*BI site by insertion mutagenesis with a double-stranded oligonucleotide to create plasmid construct pHIL-MRP1cHA-His<sub>6</sub>.

**Transformation of *P. pastoris*.** Transformation of *P. pastoris* strain GS115 (*his4*, Mut<sup>+</sup>) and KM71 (*arg4*, *his4 aox1::ARG4*, Mut<sup>s</sup>) by plasmid pHIL-MRP1cHA-His<sub>6</sub> was carried out by a lithium chloride method, as suggested by the manufacturer of the *P. pastoris* expression system (Invitrogen). Prior to transformation, the plasmids were linearized by restriction cleavage with *Not*I to facilitate homologous recombination at the *AOX1* locus. MRP1-expressing clones in GS115 were identified by their His<sup>+</sup> and Mut<sup>s</sup> growth phenotype as previously described (49, 50), and confirmed by immunoblotting analysis using anti-HA monoclonal antibody. The *P. pastoris* strain KM71 has a Mut<sup>s</sup> growth phenotype due to the presence of the *aox1::ARG4* chromosomal fusion; thus, MRP1-expressing clones in the KM71 strain were identified solely by immunoblotting using the anti-HA monoclonal antibody. The vector plasmid, pHIL-D2, was also transformed into both *P. pastoris* strains under the same conditions, and individual clones were randomly picked as negative controls.

**Membrane Preparation.** Small-scale and large-scale membrane preparations and identification of MRP1-expressing *P. pastoris* clones by immunoblotting were carried out as previously described (49, 50). To prepare membrane vesicles (MVs) for transport assays, the crude membrane pellets were resuspended in transport buffer [250 mM sucrose and 10 mM Tris-HCl (pH 7.4)], washed once with the same buffer by centrifugation (200000g at 4 °C for 60 min). The resulting pellets were resuspended in 3 mL of transport buffer, passing 20 times through a 27-gauge needle for MV formation. Aliquots of the MVs were fast-frozen in a dry ice/ethanol bath and stored at –80 °C until they were used. The protein concentration was determined using a commercially available

amido black staining reagent (Bio-Rad Laboratories, Hercules, CA) using BSA as a standard.

**Immunodetection of MRP1.** Membrane proteins (20 µg) were separated via 7.5% SDS–PAGE according to Laemmli (53). The gels were either stained with Coomassie brilliant blue R250 or blotted to nitrocellulose. Detection of MRP1 by immunoblotting was carried out as previously described (12) using an anti-HA mouse monoclonal antibody 16B12 (1:1000 dilution) or with the MRP1 specific monoclonal antibody QCRL1 (1:100 dilution). For both anti-HA and QCRL1 monoclonal antibodies, a horseradish peroxidase-conjugated sheep anti-mouse antibody was used as the secondary antibody. The immune complexes were revealed with the ECL detection system (Amersham).

**Photolabeling of MRP1 with 8-Azido[α-<sup>32</sup>P]ATP.** For direct photolabeling of MRP1, membrane proteins (20 µg) were incubated in Tris-EGTA buffer [40 mM Tris-HCl (pH 7.4, 25 °C) and 0.1 mM EGTA] containing 3 mM MgCl<sub>2</sub> and 5 µM 8-azido[α-<sup>32</sup>P]ATP on ice for 20 min, followed by a 3 min UV irradiation (λ = 260 nm, UVS-II Minerallight, model R-52, UVP Inc., San Gabriel, CA), unless otherwise specified in the figure legends. Membranes were recovered by centrifugation (245000g at 4 °C for 30 min; Beckman TLA100 rotor), washed once with 100 µL of ice-cold Tris-EGTA buffer, and dissolved in 15 µL of Laemmli buffer. Samples were incubated at 37 °C for 30 min prior to loading on a 7.5% SDS–PAGE gel. The gels were dried and subjected to autoradiography using a PhosphorImager or were exposed to Kodak X-AR films with an intensifying screen (Kodak) at –80 °C. The relative amount of radioactivity incorporated in MRP1 was quantified using the ImageQuANT software package (Molecular Dynamics, Inc., Sunnyvale, CA). Each experiment was repeated at least twice.

For vanadate-induced trapping of nucleotides in MRP1, membrane proteins (20 µg) were incubated for 10 min at 37 °C in Tris-EGTA buffer containing 3 mM MgCl<sub>2</sub> and 5 µM 8-azido[α-<sup>32</sup>P]ATP in the presence or absence of 200 µM vanadate, unless otherwise indicated in the figure legends. Reactions were stopped by chilling the tubes in an ice-cold TLA100 rotor (Beckman), and the membranes were recovered by centrifugation at 245000g at 4 °C for 30 min to remove unbound nucleotide. The pellets were washed once with ice-cold Tris-EGTA buffer and resuspended in 12 µL of the same buffer, followed by UV irradiation on ice for 5 min (λ = 260 nm) as described above. Eight microliters of Laemmli buffer was then added to each tube, and the proteins were resolved by SDS–PAGE (7.5%). The specific labeling of the MRP1 was revealed by PhosphorImaging and autoradiography, as described above.

**Photoaffinity Labeling with [<sup>125</sup>I]IAARh123.** Total membranes (20 µg) were incubated with 1 µM [<sup>125</sup>I]IAARh123 (in a total volume of 20 µL) at room temperature for 30 min in the dark as previously described (54). Membranes were then incubated for an additional 10 min on ice followed by UV irradiation at 254 nm for 10 min while on ice (Stratagene 1800 UV cross-linker, Stratagene, La Jolla, CA). For competition assays, membranes were photoaffinity labeled with 1 µM [<sup>125</sup>I]IAARh123 in the absence or presence of a molar excess of VBL, VP-16, DOX, LTC<sub>4</sub>, or MK571 as previously described (38). Following photoaffinity labeling, samples were mixed with 80 µL of buffer A [1% SDS and 50 mM Tris (pH 7.4, 25 °C)] and 320 µL of buffer B [1.25%



Triton X-100, 190 mM NaCl, and 50 mM Tris (pH 7.4, 25 °C)]. Immunoprecipitation was carried out as previously described (55) using the anti-HA monoclonal antibody. Immunoprecipitated proteins were resolved by SDS-PAGE using the Fairbanks system (56). Gels were dried and exposed to Kodak X-AR film at -80 °C.

**Vesicle Transport of [<sup>3</sup>H]LTC<sub>4</sub>.** ATP-dependent uptake of [<sup>3</sup>H]LTC<sub>4</sub> into membrane vesicles was assessed by rapid filtration, as described previously (5, 15), with the following modifications. Standard transport assays were carried out at room temperature in a reaction mixture (20 μL per reaction) containing 20 μg of MVs, 4 mM ATP, 10 mM MgCl<sub>2</sub>, an ATP-regenerating system consisting of 10 mM creatine phosphate and 100 μg/mL creatine kinase, and 50 nM [<sup>3</sup>H]-LTC<sub>4</sub> (14.6 nCi per 20 μL reaction) with MVs added last to initiate the transport reaction (final volume of 110 μL for the time course assay). Modifications of the conditions are described in the figure legends. Aliquots of 20 μL of reaction mixture were removed after incubation for 30 s and 1, 2, 3, and 5 min, diluted in 1 mL of ice-cold transport buffer, and filtered immediately through a nitrocellulose filter (0.2 μm, Whatman International Ltd., Maidstone, England) on a Millipore 25 mm glass microanalysis filtration manifold (Fisher Scientific, Montreal, PQ) under vacuum. Filters were rinsed twice with 5 mL of ice-cold transport buffer. The amount of radioactivity on the filters was determined by liquid scintillation counting. The level of MRP1-dependent [<sup>3</sup>H]LTC<sub>4</sub> transport into MVs was calculated by subtracting the amount of MVs-associated radioactivity obtained in the presence of AMP from that obtained in the presence of ATP. The concentration-dependent transport of LTC<sub>4</sub> in MRP1 MVs was analyzed by incubation in increasing concentrations of [<sup>3</sup>H]LTC<sub>4</sub> (from 6.25 to 100 nM) in the presence of ATP and an ATP-regenerating system at room temperature for 5 min. All the experiments were performed in triplicate.

## RESULTS

**Expression of MRP1 in *P. pastoris*.** Plasmid construct pHIL-MRP1cHA-His<sub>6</sub> was used to transform *P. pastoris* strains GS115 and KM71. His<sup>+</sup> transformants were selected and screened for expression of the HA epitope-tagged MRP1 by immunoblotting with the mouse monoclonal anti-HA antibody 16B12. Clones positive for MRP1 expression were identified at a frequency between 10 (KM71) and 20% (GS115) of His<sup>+</sup> transformants, and large differences in the levels of protein expression were noted in independent clones (data not shown). In general, the level of MRP1 expression was higher in KM71 than in GS115 transformants. In all cases, the MRP1 expressed in these clones was immunoreactive with both anti-HA (Figure 1A) and anti-MRP1 (QCRL-1) (Figure 1B) monoclonal antibodies, and migrated with an apparent molecular mass of 165 kDa (lanes 2 and 3), a size compatible to that predicted from the MRP1 cDNA sequence (57), but smaller than the 190 kDa MRP1 overexpressed in mammalian cell transfectants as previously reported (51, 57), and as shown in panels A and B of Figure 1 (lanes 1). Treatment of MRP1-expressing *P. pastoris* membrane fractions with PNGase F did not alter the size of the immunoreactive MRP1 (data not shown), suggesting that MRP1 expressed in yeast is underglycosylated by contrast to MRP1 expressed in mammalian cells (51, 57). Importantly, the amount of recombinant immunoreactive MRP1 expressed

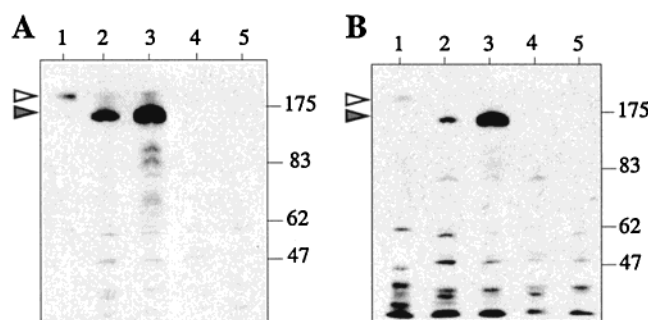


**FIGURE 1:** Immunodetection of MRP1 by Western blotting analysis with anti-HA (A) and QCRL-1 anti-MRP1 monoclonal antibodies (B). Crude membrane proteins (20 μg) were dissolved in 15 μL of Laemmli sample buffer (53), separated by SDS-PAGE (7.5%), and transferred to nitrocellulose as described in Materials and Methods: lane 1, crude plasma membranes from HeLa/MRP1-HA cells (containing one HA epitope tag at amino acid residue 1222 in MRP1) selected in VP16 (250 ng/mL) (12) as a positive control; lane 2, GS115/MRP1cHA-His<sub>6</sub>; lane 3, KM71/MRP1cHA-His<sub>6</sub>; lane 4, GS115/pHIL-D2; and lane 5, KM71/pHIL-D2. The molecular mass standards (in kilodaltons) are shown on the right side. The open arrowheads identify MRP1 expressed in HeLa cells, and the closed arrowheads indicate MRP1 expressed in *P. pastoris* cells.

by either GS115 or KM71 transformants was far greater than that expressed by mutildrug-resistant HeLa/MRP1 transfectants (Figure 1A,B). These results indicate that MRP1 can be abundantly and stably expressed in two strains of *P. pastoris*. For the rest of the experiments, the KM71/MRP1 clone shown in lanes 3 of Figure 1 and expressing high levels of MRP1 was used throughout.

**8-Azido[α-<sup>32</sup>P]ATP Binding to MRP1 Expressed in *P. pastoris*.** MRP1 has two predicted NBDs, and has been shown to bind and hydrolyze ATP in mammalian cells (41, 42, 44, 58). These two properties were investigated for MRP1 expressed in yeast cells. To examine whether the MRP1 expressed in *P. pastoris* can bind ATP, a direct photolabeling assay with 8-azido[α-<sup>32</sup>P]ATP was performed. Crude membrane fractions from control and MRP1-expressing cells were incubated on ice with 8-azido[α-<sup>32</sup>P]ATP in the presence of Mg<sup>2+</sup>, followed by UV cross-linking and analysis of the photolabeled products by SDS-PAGE and autoradiography (Figure 2A). A photolabeled species of 165 kDa is evident in membranes from MRP1-expressing cells but is absent in membranes from plasmid vector-transformed cells. The size of the photolabeled species corresponds to the size of the MRP1 detected by immunoblotting the same fractions with anti-MRP1 and anti-HA antibodies (Figure 1). Moreover, the amount of photolabeling of MRP1 in these fractions increased with the amount of membrane protein introduced in the photolabeling reactions (Figure 2A). These observations suggest that the MRP1 expressed in *P. pastoris* can bind to 8-azido[α-<sup>32</sup>P]ATP. The requirement of Mg<sup>2+</sup> ions for 8-azido[α-<sup>32</sup>P]ATP binding to MRP1 was investigated by varying the concentration of Mg<sup>2+</sup> ions and EDTA in the photolabeling reactions (Figure 2B). Under control conditions (absence of added Mg<sup>2+</sup> and EDTA), MRP1 was only weakly photolabeled, and addition of 1 mM EDTA abolished this reactivity. Increasing amounts of Mg<sup>2+</sup> ions, in the presence of 1 mM EDTA, resulted in an increased level of photolabeling by 8-azido[α-<sup>32</sup>P]ATP in a concentration-dependent fashion. Conversely, maintaining the Mg<sup>2+</sup> concentration at

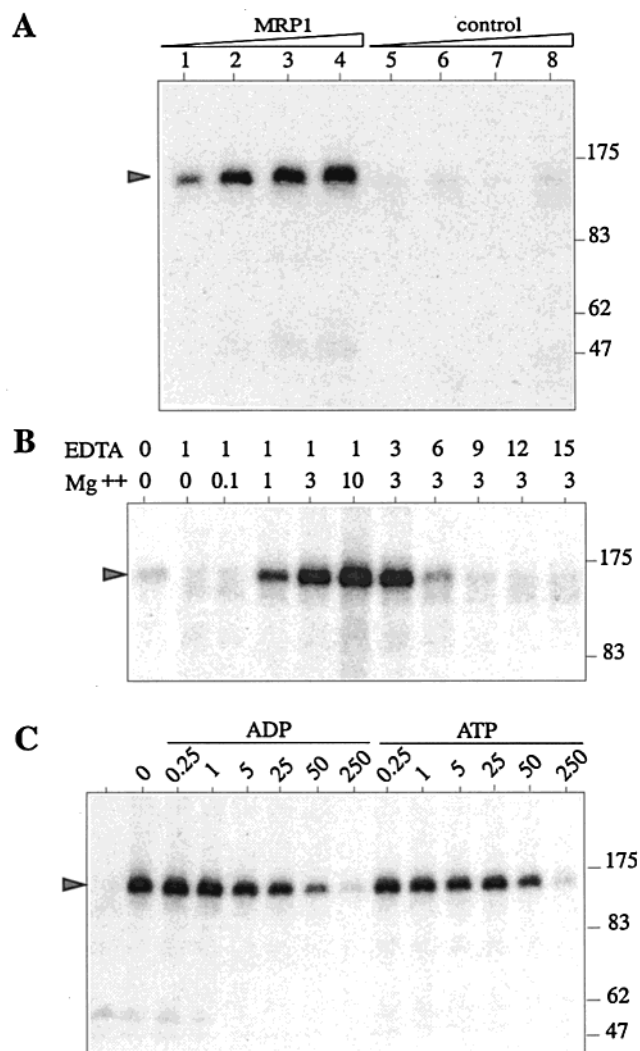


**FIGURE 2:** Direct photolabeling of MRP1 with 8-azido[ $\alpha$ - $^{32}$ P]ATP. Membrane proteins (20  $\mu$ g) were incubated in the labeling buffer on ice for 10 min prior to the addition of 5  $\mu$ M ice-cold 8-azido[ $\alpha$ - $^{32}$ P]ATP and photolabeling. The photolabeled proteins were separated by SDS-PAGE (7.5%) and analyzed by autoradiography. Radiolabeled MRP1s are indicated by arrowheads. (A) Increasing amounts of membrane proteins from KM71/MRP1cHA-His<sub>6</sub> cells (lanes 1–4) and control KM71/pHIL-D2 cells (lanes 5–8) were used in the photolabeling reactions: lanes 1 and 5, 10  $\mu$ g; lanes 2 and 6, 20  $\mu$ g; lanes 3 and 7, 30  $\mu$ g; and lanes 4 and 8, 40  $\mu$ g. (B) Requirement of Mg<sup>2+</sup> in direct photolabeling of MRP1 with 8-azido[ $\alpha$ - $^{32}$ P]ATP. Membranes were incubated with EDTA (1 mM) at room temperature (RT) for 10 min, and then increasing concentrations of MgCl<sub>2</sub> were added to the mixture and incubated for an additional 10 min at RT. Tubes were transferred on ice for 10 min prior to the addition of ice-cold radiolabeled nucleotide and photolabeling. In the lanes where the Mg<sup>2+</sup> concentration remains constant, the order of addition of EDTA and MgCl<sub>2</sub> was reversed. All concentrations of EDTA and Mg<sup>2+</sup> are in millimolar. (C) Increasing concentrations of ADP or ATP (shown on the top of the figure, in micromolar) were added to ice-cold reaction mixtures prior to the addition of 8-azido[ $\alpha$ - $^{32}$ P]ATP and photolabeling. All the reactions were carried out in 3 mM Mg<sup>2+</sup> except in lane 1 (no Mg<sup>2+</sup>, 1 mM EDTA).

3 mM, while increasing the molar excess of EDTA, progressively abolished photolabeling of MRP1 (Figure 2B). These results suggest that Mg<sup>2+</sup> is required for the binding of 8-azido[ $\alpha$ - $^{32}$ P]ATP to MRP1. The nucleotide binding specificity of MRP1 expressed in *P. pastoris* was investigated in competition assays, using cold ATP and ADP as competing

ligands incorporated in the labeling reactions. Both ADP and ATP were able to inhibit MRP1 photolabeling by 8-azido[ $\alpha$ - $^{32}$ P]ATP, indicating that ADP and ATP can both be accommodated in the nucleotide binding sites of MRP1 (Figure 2C). Fifty percent inhibition occurred at concentrations ranging from 50 to 100  $\mu$ M, or from a 10 to 20-fold molar excess of labeled ligand (kept at 5  $\mu$ M). Finally, the effect of known substrates of MRP1 such as chemotherapeutic agents (VP16, VBL, and VCR), as well as glutathione (GSH and GSSH) and glucuronide conjugates, on direct photolabeling of MRP1 with 8-azido[ $\alpha$ - $^{32}$ P]ATP was examined. No significant increase or decrease in the level of 8-azido[ $\alpha$ - $^{32}$ P]ATP binding to MRP1 was seen over a broad range of substrate concentrations (data not shown).

**Vanadate-Induced 8-Azido[ $\alpha$ - $^{32}$ P]ATP Trapping in MRP1 Expressed in *P. pastoris*.** In the case of ABC transporters such as P-gp and MRP1, ATP hydrolysis generates a high-energy protein–MgADP–P<sub>i</sub> intermediate proposed to underlie a major structural change in the protein, including modulation of the protein affinity for substrates. In the presence of P<sub>i</sub> analogues such as V<sub>i</sub>, P<sub>i</sub> is replaced with V<sub>i</sub> in the active site, leading to the formation of a stably inhibited protein–MgADP–V<sub>i</sub> complex (59). P-gp and MRP1 can both hydrolyze 8-azido-ATP, and thus, the vanadate-inhibited state can be visualized by photo-cross-linking the azido group of 8-azido[ $\alpha$ - $^{32}$ P]ATP to the protein. Indeed, vanadate-induced trapping of the nucleotide has been used as an indicator of ATPase activity by MRP1 expressed in mammalian cells (40, 44). Thus, the ATPase activity of MRP1 expressed in *P. pastoris* was tested by its ability to trap 8-azido[ $\alpha$ - $^{32}$ P]nucleotides in a vanadate-dependent fashion. Membranes from control and MRP1-expressing *P. pastoris* cells were incubated with 8-azido[ $\alpha$ - $^{32}$ P]ATP (5  $\mu$ M) in the presence or absence of orthovanadate at 37 °C for 10 min (hydrolysis conditions). The protein–MgADP–V<sub>i</sub> complexes were then washed off unincorporated nucleotides by centrifugation, followed by UV cross-linking and SDS-PAGE (Figure 3). Results in Figure 3A show that under these conditions, the 165 kDa MRP1 can be specifically labeled in membranes from *P. pastoris*/MRP1 cells, and this complex is absent from membranes of control cells. The presence of both Mg<sup>2+</sup> ions and orthovanadate is required for the azidonucleotide trapping in MRP1, and the level of MRP1 photolabeling increases with increasing concentrations of orthovanadate (Figure 3B). Increasing the concentration of 8-azido[ $\alpha$ - $^{32}$ P]ATP from 5 to 40  $\mu$ M results in an increased level of photolabeling of the MRP1 (Figure 3C). Therefore, MRP1 expressed in *P. pastoris* can form the inhibited protein–MgADP–V<sub>i</sub> complex, a behavior consistent with the presence of ATPase activity in the recombinant MRP1.

Previous studies in mammalian cells have shown that ATP hydrolysis by MRP1 can be stimulated by certain transported substrates, including several anti-cancer drugs (41, 42). Therefore, the effect of VBL, VCR, paclitaxel (TXL), and VP16, as well as LTC<sub>4</sub>, on vanadate-induced nucleotide trapping in MRP1 was examined. Moreover, the effect of the LTD<sub>4</sub> receptor antagonist MK571, previously shown to inhibit MRP1-mediated LTC<sub>4</sub> transport (15) and MRP1 photoaffinity labeling by quinoline-based drugs (37), was also analyzed. Among the chemotherapeutic drugs that were tested, all but VP16 exhibited concentration-dependent stimulation of vanadate-induced nucleotide trapping by

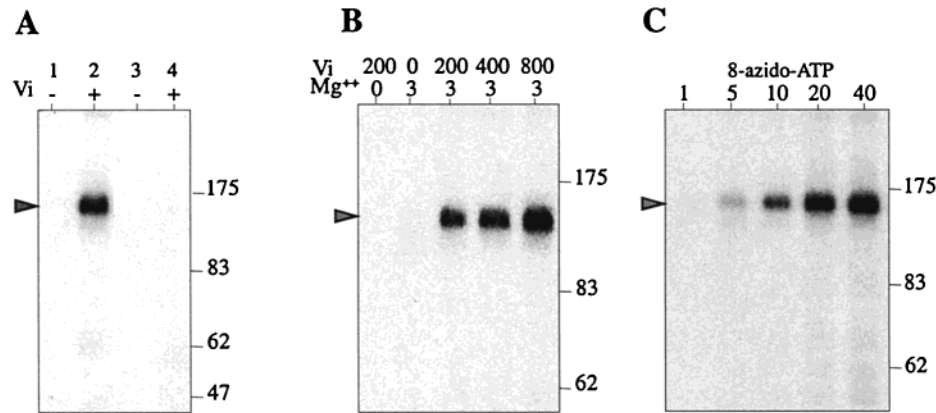


FIGURE 3: Orthovanadate-induced nucleotide trapping by MRP1. (A) Membrane proteins from KM71/MRP1cHA-His<sub>6</sub> (lanes 1 and 2) and KM71/pHIL-D2 (lanes 3 and 4) cells were incubated with 5 μM 8-azido[α-<sup>32</sup>P]ATP and 3 mM Mg<sup>2+</sup> at 37 °C for 10 min, in the absence (lanes 1 and 3) and presence (lanes 2 and 4) of 200 μM orthovanadate (V<sub>i</sub>), followed by photo-cross-linking and SDS-PAGE. (B) Membrane proteins from the KM71/MRP1cHA-His<sub>6</sub> cells were incubated with 8-azido[α-<sup>32</sup>P]ATP at 37 °C for 10 min, in varying concentrations of V<sub>i</sub> (in micromolar) and Mg<sup>2+</sup> (in millimolar). (C) Membrane proteins from the KM71/MRP1cHA-His<sub>6</sub> cells were photolabeled in increasing concentrations of 8-azido[α-<sup>32</sup>P]ATP (in micromolar). In all cases, 20 μg of membrane proteins was used in each reaction, and radiolabeled MRP1 is indicated by the arrowhead.

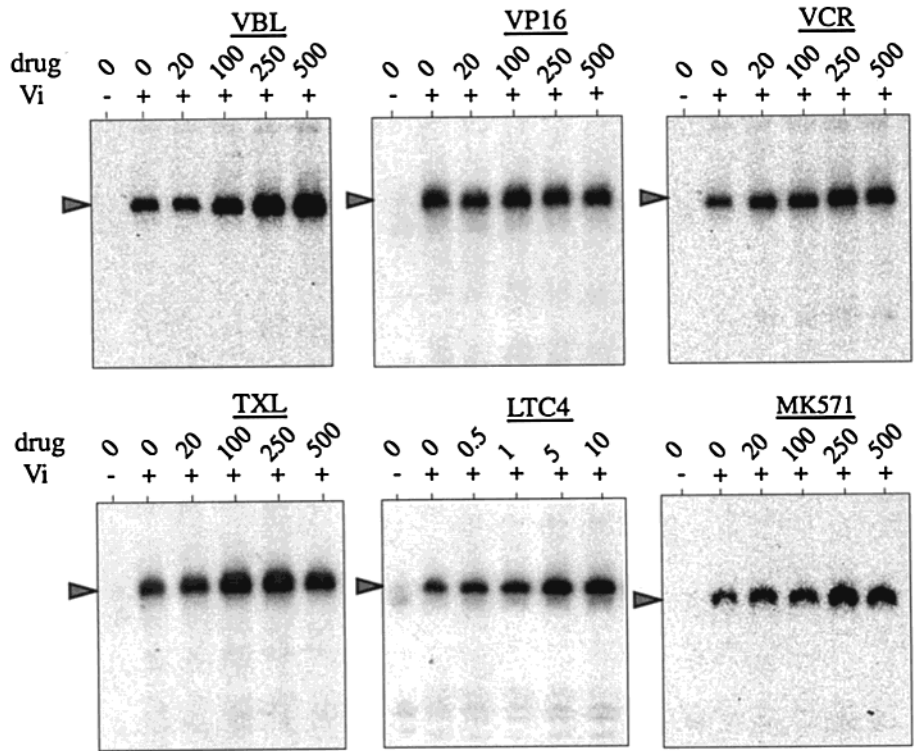


FIGURE 4: Stimulation of vanadate-induced nucleotide trapping in MRP1. Membrane proteins (20 μg) from the KM71/MRP1cHA-His<sub>6</sub> cells were incubated with increasing concentrations of VBL, VP16, VCR, TXL, LTC<sub>4</sub>, and MK571 (in micromolar) for 10 min at room temperature prior to the addition of 5 μM 8-azido[α-<sup>32</sup>P]ATP and photolabeling. The reactions were carried out under hydrolysis conditions as described in Materials and Methods. The presence or absence of vanadate in the reactions is indicated. The radiolabeled MRP1 in autoradiograms is indicated by the arrowhead.

MRP1 (Figure 4). Likewise, LTC<sub>4</sub> and to a lesser extent MK571 also stimulated nucleotide trapping in MRP1 (Figure 4). Quantitative analysis (using ImageQuaNT software) indicated that the level of stimulation of photolabeling ranged from 1.5- to 3-fold (data not shown), a behavior similar to that reported for MRP1 expressed in mammalian cells (40). Conversely, doxorubicin (DOX) showed an inhibitory effect on the vanadate-induced nucleotide trapping by MRP1 (data not shown). These results indicate that MRP1 expressed in yeast cells displays substrate-modulated ATPase activity.

*Photoaffinity Labeling of MRP1 with [<sup>125</sup>I]IAARh123.* We have previously shown that MRP1 overexpressed in multi-

drug-resistant H69/AR cells and HeLa/MRP1 transfectants can be photolabeled by analogues of quinoline-based drugs (37), as well as by a photoactive analogue of rhodamine 123, [<sup>125</sup>I]IAARh123 (38). To determine if MRP1 expressed in yeast retains its ability to interact with these compounds, membranes from control and MRP1-expressing cells were incubated with [<sup>125</sup>I]IAARh123 followed by UV cross-linking and analysis by SDS-PAGE and autoradiography (Figure 5). The probe was found to label a number of proteins in membrane fractions from both control and MRP1-expressing cells; however, a specific polypeptide of 165 kDa was uniquely labeled in MRP1 membranes (Figure 5A, left



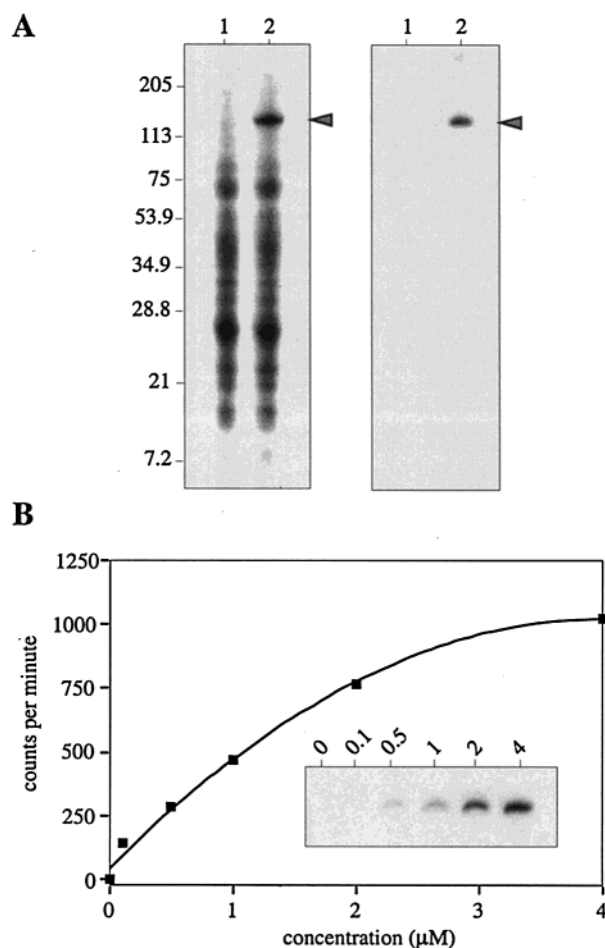


FIGURE 5: Photoaffinity labeling of MRP1 by [ $^{125}$ I]IAARh123. (A) Autoradiogram of the photoaffinity labeling reaction of membrane proteins (20  $\mu$ g) from control KM71/pHIL-D2 (lane 1) or KM71/MRP1cHA-His<sub>6</sub> (lane 2) cells with 1  $\mu$ M [ $^{125}$ I]IAARh123 as described in Materials and Methods. The reaction mixtures were analyzed either directly by SDS-PAGE (left panel) or after immunoprecipitation of MRP1 with anti-HA monoclonal antibody prior to SDS-PAGE (right panel). Photoaffinity-labeled MRP1 is indicated by the arrowhead. (B) Quantitative representation of the photoaffinity labeling of MRP1 with increasing concentrations of [ $^{125}$ I]IAARh123. Quantification of the labeled MRP1 band was carried out with ImageQuANT, and the results were plotted against the concentrations of ligand that were used.

panel). The identity of this photoaffinity-labeled protein as MRP1 was confirmed by immunoprecipitation of labeled membranes using the anti-HA monoclonal antibody (Figure 5A, right panel). Photolabeling of MRP1 by [ $^{125}$ I]IAARh123 in these membranes was specific, concentration-dependent, and saturable at approximately 4  $\mu$ M (Figure 5B). Finally, photolabeling by [ $^{125}$ I]IAARh123 could be competed by a series of substrates and inhibitors of MRP1 such as VBL, VP16, DOX, LTC<sub>4</sub>, and MK571. Competition of photolabeling of MRP1 was by a factor of 30–75%, depending on the compound being tested (Figure 6A,B), a behavior typical of that observed for MRP1 expressed in mammalian cell membranes (37, 38). These results suggest that the MRP1 expressed in *P. pastoris* is able to interact with its drug substrates and modulators.

**ATP-Dependent Uptake of [ $^3$ H]LTC<sub>4</sub> by MRP1 Membrane Vesicles.** To determine if MRP1 expressed in *P. pastoris* is fully functional and transport-competent, we tested its ability

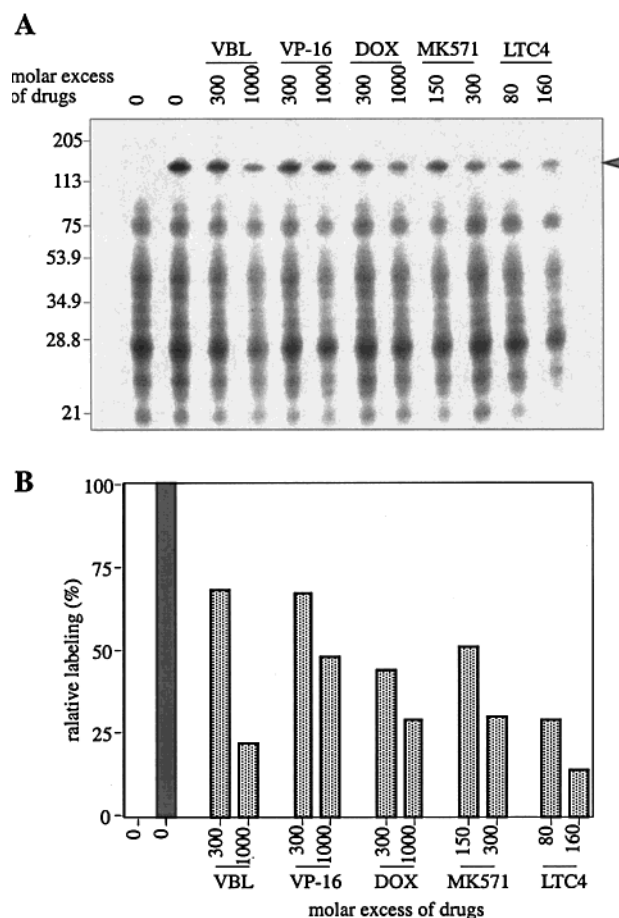


FIGURE 6: Competition of photoaffinity labeling of MRP1 by [ $^{125}$ I]IAARh123. The photoaffinity labeling reactions were carried out in the absence or presence of a molar excess of various MRP1 substrates, VBL, VP16, DOX, MK571, and LTC<sub>4</sub>, as described in the legend of Figure 5. (A) Autoradiogram of the total labeled proteins. The first lane shows a reaction carried out with membrane proteins from the control KM71/pHIL-D2 cells, while all others were from KM71/MRP1cHA-His<sub>6</sub> cells. The photolabeled MRP1 is pointed out by an arrowhead. (B) Quantification of the MRP1 photolabeled by [ $^{125}$ I]IAARh123 in panel A, using ImageQuANT. The relative signal of MRP1 in the absence of competitors (control in lane 2) was set at 100%, and the effect of competing ligands on MRP1 labeling is presented as a histogram (hatched boxes) showing the relative amount of remaining signal in MRP1.

to transport [ $^3$ H]LTC<sub>4</sub>. LTC<sub>4</sub> has been shown to be a high-affinity substrate for MRP1, and has been used to monitor MRP1 transport activity in membrane vesicles prepared from mammalian cells (5, 15). For this, MVs were prepared from either control or MRP1-expressing *P. pastoris* cells and incubated with [ $^3$ H]LTC<sub>4</sub> in the presence of either ATP or AMP, and the level of MVs-associated radioactivity was monitored over time by a rapid filtration assay (Figure 7A). MRP1 expression in MVs from *P. pastoris* cells caused a robust, rapid, and ATP-dependent accumulation of [ $^3$ H]LTC<sub>4</sub> when compared to that in MVs from the control cells, which remained low over time. Accumulation of [ $^3$ H]LTC<sub>4</sub> in MRP1-positive MVs was specific, and the level increased in a concentration-dependent fashion with respect to ligand (Figure 7B), with a linear relationship observed over the concentration range that was tested (estimated  $K_m \approx 85$  nM). Finally, MRP1-stimulated accumulation of [ $^3$ H]LTC<sub>4</sub> into MVs was strictly temperature-dependent, suggesting that it was due to active transport as opposed to an increased level

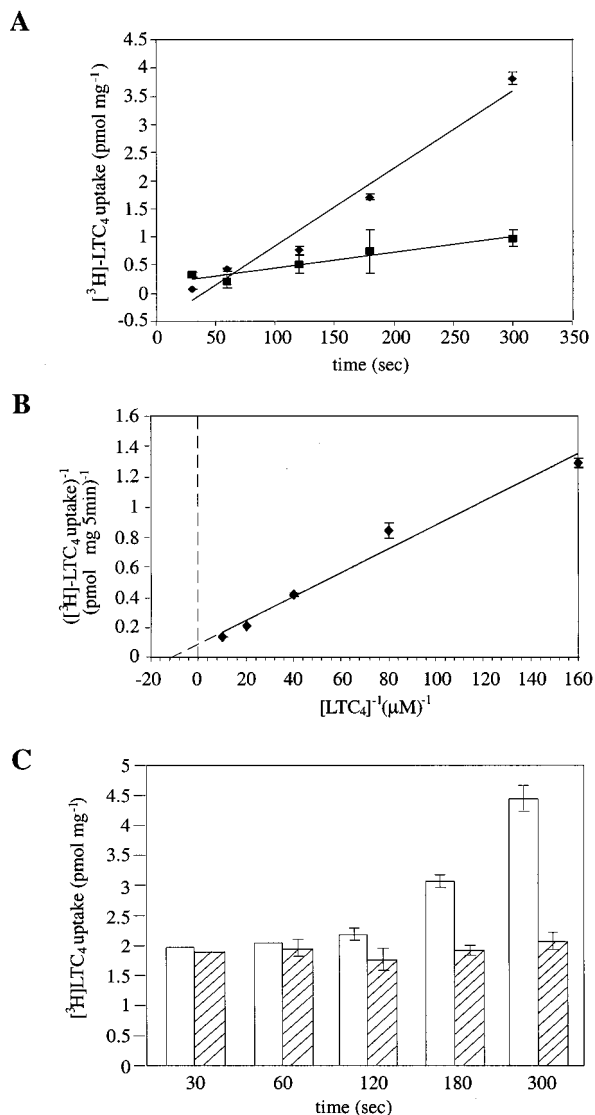


FIGURE 7: ATP-dependent  $\text{LTC}_4$  transport by MRP1-containing membrane vesicles. (A) Time course of  $[^3\text{H}]\text{LTC}_4$  uptake by MVs from KM71/MRP1cHA-His<sub>6</sub> (◆) and vector-transformed cells (■). MVs were incubated with 50 nM  $[^3\text{H}]\text{LTC}_4$  in the presence of ATP or AMP (4 mM each), 10 mM  $\text{MgCl}_2$ , and an ATP regeneration system as described in Materials and Methods. Each value is obtained by subtracting the amount of radioactivity associated with the presence of AMP from that associated with the presence of ATP. (B) Kinetic analysis on MRP1-containing MVs-mediated  $\text{LTC}_4$  uptake with the  $\text{LTC}_4$  concentration ranging from 6.25 to 100 nM as described in Materials and Methods. Data transformation to kinetic parameters was performed by Lineweaver–Burk regression analysis. (C) Uptake of  $\text{LTC}_4$  by MRP1-containing MVs in the presence of 4 mM ATP at room temperature (open bars) or on ice (hatched bars) as described in Materials and Methods. All data represent mean values of triplicates in a single determination. Standard deviations (SD) are shown as error bars.

of ligand binding to MRP1-positive MVs (Figure 7C). Together, these results indicate that MRP1 expressed in *P. pastoris* is transport-competent.

## DISCUSSION

We have successfully overexpressed a recombinant human MRP1 in the methylotrophic yeast *P. pastoris*. The protein is expressed as a 165 kDa polypeptide which does not appear to be glycosylated, a phenomenon we have previously noted for another ABC transporter, P-gp, expressed in *P. pastoris*

cells (49). The protein is stable and expressed in the membrane fraction of these yeast cells. Despite the apparent underglycosylated status of MRP1 in yeast cells, the protein shows biochemical properties that are undistinguishable from those of the protein expressed in mammalian cells. Studies by photolabeling with 8-azido[ $\alpha$ - $^{32}\text{P}$ ]ATP, with 8-azido[ $\gamma$ - $^{32}\text{P}$ ]ATP (43, 44, 46), or with purified MRP1 reconstituted in lipids (41, 42, 45) have shown that MRP1 can bind and hydrolyze ATP. MRP1 expressed in yeast membranes binds ATP as shown by photolabeling studies with 8-azido[ $\alpha$ - $^{32}\text{P}$ ]ATP under binding conditions (incubation on ice). In addition, this photolabeling can be further stimulated by vanadate, upon incubation at 37 °C, showing that MRP1 can also hydrolyze ATP. Using  $V_i$ -induced trapping of 8-azido[ $\alpha$ - $^{32}\text{P}$ ]ATP into the protein, we further observed that ATP hydrolysis by MRP1 can be further stimulated by MRP1 substrates such as VBL, VCR, TXL,  $\text{LTC}_4$ , and the  $\text{LTD}_4$  receptor antagonist MK571. Stimulation of MRP1-mediated ATP hydrolysis as measured by the level of vanadate-induced nucleotide trapping by chemotherapeutic drugs, such as VBL, VCR, and TXL, is consistent with the results obtained by Taguchi et al. (40) and Chang et al. (41). Since neither VBL nor TXL is a transport substrate for MRP1, these results suggest that they may nevertheless act at a common binding site on MRP1 to stimulate ATP hydrolysis. This situation is reminiscent of another ABC transporter, P-gp, where substrates or inhibitors that are transported or not transported by the protein appear to share both a common binding site on the protein and an ability to stimulate its ATPase activity. Interestingly, VP16 exhibited only a marginal effect on MRP1-mediated nucleotide trapping in our study, differing from the results obtained by Nagata et al., who observed a prominent 4-fold and, in the presence of glutathione, a 20-fold stimulation on nucleotide trapping by VP16 (46). The source of this apparent discrepancy remains unknown but may be due to differences in the experimental systems that were used. In particular, MRP1 was tested in two different membrane systems, one from multidrug-resistant human KB carcinoma cells and the other from *P. pastoris*, which may differ in biochemical compositions, including lipid composition and cholesterol that may modulate ATPase activity. In addition, glutathione was not added in our assay, and concentrations of VP16 analyzed in our study were lower than that tested by Nagata et al. (46). Stimulation of MRP1-mediated nucleotide trapping by  $\text{LTC}_4$  in the yeast membranes is a reported hallmark of MRP1 ATPase activity monitored both in mammalian and insect cell membranes (42). The inhibitory effect of DOX on MRP1-mediated nucleotide trapping is in contrast to the observation made by Taguchi et al. (40). The reason for this discrepancy is currently unknown. Moreover, MRP1 expressed in yeast retains its ability to bind the photoactivatable drug analogue [ $^{125}\text{I}$ ]IAARh123. Competition experiments with known MRP1 substrates and inhibitors suggest very similar substrate binding properties of MRP1 expressed in *P. pastoris* when compared to those of MRP1 present in mammalian cells, and as previously established by our group (38). Finally, membrane vesicles from MRP1-overexpressing yeast are able to transport  $\text{LTC}_4$  in an ATP-dependent fashion, with a  $K_m$  value (85 nM) comparable to that for MRP1 expressed in mammalian cells (97–105 nM) (5, 15). Therefore, MRP1 expressed in yeast shows biochemical and functional char-



acteristics with respect to substrate binding, ATP binding and hydrolysis, and ATP-dependent substrate transport very similar to those reported for the protein expressed in mammalian cell membranes.

Of particular interest is the observation in *P. pastoris*/MRP1 membranes that 8-azido[ $\alpha$ - $^{32}$ P]ATP binding by MRP1 (on ice) is dependent upon the presence of  $Mg^{2+}$  ions and is inhibited by EDTA (Figure 2B). This result is highly reproducible, and suggests a behavior clearly different from that of P-gp expressed in the same system, where ATP binding by the protein is largely insensitive to the presence of added  $Mg^{2+}$  (60). However, this observation is consistent with results recently reported by Hou et al. (44), who showed that photolabeling of MRP1 in mammalian BHK cell membranes by 8-azido[ $\gamma$ - $^{32}$ P]ATP is inhibited by EDTA and strongly stimulated by vanadate. We did not observe any stimulation on the 8-azido[ $\alpha$ - $^{32}$ P]ATP binding to MRP1 in the presence of vanadate, probably because of the low temperature (incubation on ice instead of at 37 °C) used for binding reactions. These authors proposed a model involving allosteric interactions between two nonequivalent NBDs, in which ATP hydrolysis at one site may stimulate ATP binding at the other site (44). Although the strict dependence of  $Mg^{2+}$  for ATP binding by MRP1 may also reflect a very low-affinity site requiring  $Mg^{2+}$  for stabilization of ATP, this unique behavior in MRP1 has been preserved for the recombinant protein expressed in yeast cells.

MRP1 is a large integral membrane protein consisting of a minimum of 17 TM domains clustered in three hydrophobic membrane-associated regions (12, 13). A clear understanding of the mechanism of action of the protein, including recognition of a large group of structurally unrelated substrates, the mechanism of ATP hydrolysis, and coupling of ATP hydrolysis to drug transport all require high-resolution structural information in a dynamic fashion. Such information can be obtained by methods such as fluorescence spectroscopy of endogenous or introduced tryptophan (61, 62) or modified cysteines (63, 64), infrared spectroscopy (65, 66), and ultimately X-ray crystallography (67). All these methods require large amounts of highly pure and active proteins. So far, MRP1 has been purified in small quantities from BHK cells (41) and H69AR cells (42). Protein preparations of good purity have been obtained from these cells, but such purification schemes are expensive and the amounts obtained small. In addition, MRP1 purified from either BHK cells (44) or H69AR cells (42) shows dramatic differences in ATPase activity with respect to  $K_m$  (3 vs 0.1 mM) and  $V_{max}$  [460 vs 1.5 nmol min $^{-1}$  (mg of protein) $^{-1}$ ], and stimulation by drugs. The successful expression of MRP1 in *P. pastoris* cells reported here is an alternative and relatively inexpensive method for the expression and purification of MRP1 in large amounts. Results in Figure 1 show that *P. pastoris* expresses between 10- and 40-fold more MRP1 than multidrug-resistant HeLa/MRP1 transfectants. Thus, the relatively large levels of MRP1 expression in *P. pastoris*, together with the relative ease with which large amounts of yeast cells can be generated, should facilitate the isolation of large amounts of the pure recombinant protein.

Recently, we have reported on the expression and purification of recombinant biotinylated P-glycoprotein (mouse Mdr3) from *P. pastoris* (68). This simple method is based

on detergent extraction of Mdr3 containing a polyhistidine tail and a biotinylation domain, followed by successive affinity chromatography on Ni-NTA and avidin columns. The protein is highly pure and fully active, and it is currently used for structural studies by mass spectroscopy, infrared spectroscopy, and fluorescence spectroscopy. Preliminary results indicate that MRP1 can be purified to homogeneity using a modification of this protocol (data not shown). Therefore, the *P. pastoris* expression system may prove to be very advantageous for gaining information about the structure of MRP1 and other members of the MRP family.

## ACKNOWLEDGMENT

We are indebted to Drs. M. Julien and C. Kast for helpful suggestions during this work and for comments on this manuscript and Dr. S. P. Cole (Queen's University, Kingston, ON) for critical comments and helpful discussion during this work.

## REFERENCES

- Ambudkar, S. V., Dey, S., Hrycyna, C. A., Ramachandra, M., Pastan, I., and Gottesman, M. M. (1999) *Annu. Rev. Pharmacol. Toxicol.* 39, 361–98.
- Hipfner, D. R.; Deeley, R. G., and Cole, S. P. (1999) *Biochim. Biophys. Acta* 1461, 359–76.
- Ruetz, S., and Gros, P. (1994) *Trends Pharmacol. Sci.* 15, 260–3.
- Jedlitschky, G., Leier, I., Buchholz, U., Barnouin, K., Kurz, G., and Keppler, D. (1996) *Cancer Res.* 56, 988–94.
- Loe, D. W., Almquist, K. C., Deeley, R. G., and Cole, S. P. (1996) *J. Biol. Chem.* 271, 9675–82.
- Szczypka, M. S., Wemmie, J. A., Moye-Rowley, W. S., and Thiele, D. J. (1994) *J. Biol. Chem.* 269, 22853–7.
- Tommasini, R., Evers, R., Vogt, E., Mornet, C., Zaman, G. J., Schinkel, A. H., Borst, P., and Martinoia, E. (1996) *Proc. Natl. Acad. Sci. U.S.A.* 93, 6743–8.
- Katzmann, D. J., Hallstrom, T. C., Voet, M., Wysock, W., Golini, J., Volckaert, G., and Moye-Rowley, W. S. (1995) *Mol. Cell. Biol.* 15, 6875–83.
- Ortiz, D. F., St. Pierre, M. V., Abdulmessih, A., and Arias, I. M. (1997) *J. Biol. Chem.* 272, 15358–65.
- Aguilar-Bryan, L., Nichols, C. G., Wechsler, S. W., Clement, J. P. t., Boyd, A. E., III, Gonzalez, G., Herrera-Sosa, H., Nguy, K., Bryan, J., and Nelson, D. A. (1995) *Science* 268, 423–6.
- Inagaki, N., Gono, T., Clement, J. P., Wang, C. Z., Aguilar-Bryan, L., Bryan, J., and Seino, S. (1996) *Neuron* 16, 1011–7.
- Kast, C., and Gros, P. (1997) *J. Biol. Chem.* 272, 26479–87.
- Kast, C., and Gros, P. (1998) *Biochemistry* 37, 2305–13.
- Keppler, D., Leier, I., and Jedlitschky, G. (1997) *Biol. Chem.* 378, 787–91.
- Leier, I., Jedlitschky, G., Buchholz, U., Cole, S. P., Deeley, R. G., and Keppler, D. (1994) *J. Biol. Chem.* 269, 27807–10.
- Muller, M., Meijer, C., Zaman, G. J., Borst, P., Scheper, R. J., Mulder, N. H., de Vries, E. G., and Jansen, P. L. (1994) *Proc. Natl. Acad. Sci. U.S.A.* 91, 13033–7.
- Loe, D. W., Almquist, K. C., Cole, S. P., and Deeley, R. G. (1996) *J. Biol. Chem.* 271, 9683–9.
- Zaman, G. J., Versantvoort, C. H., Smit, J. J., Eijds, E. W., de Haas, M., Smith, A. J., Broxterman, H. J., Mulder, N. H., de Vries, E. G., Baas, F., et al. (1993) *Cancer Res.* 53, 1747–50.
- Loe, D. W., Deeley, R. G., and Cole, S. P. (1996) *Eur. J. Cancer* 32A, 945–57.
- Borst, P., Evers, R., Kool, M., and Wijnholds, J. (2000) *J. Natl. Cancer Inst.* 92, 1295–302.
- Borst, P., Evers, R., Kool, M., and Wijnholds, J. (1999) *Biochim. Biophys. Acta* 1461, 347–57.

22. Kool, M., de Haas, M., Scheffer, G. L., Scheper, R. J., van Eijk, M. J., Juijn, J. A., Baas, F., and Borst, P. (1997) *Cancer Res.* 57, 3537–47.
23. Kool, M., van der Linden, M., de Haas, M., Baas, F., and Borst, P. (1999) *Cancer Res.* 59, 175–82.
24. Paulusma, C. C., and Oude Elferink, R. P. (1997) *J. Mol. Med.* 75, 420–8.
25. Keppler, D., Leier, I., Jedlitschky, G., and Konig, J. (1998) *Chem.-Biol. Interact.* 111–112, 153–61.
26. Ito, K., Fujimori, M., Nakata, S., Hama, Y., Shingu, K., Kobayashi, S., Tsuchiya, S., Kohno, K., Kuwano, M., and Amano, J. (1998) *Oncol. Res.* 10, 99–109.
27. Kartenbeck, J., Leuschner, U., Mayer, R., and Keppler, D. (1996) *Hepatology* 23, 1061–6.
28. Paulusma, C. C., Kool, M., Bosma, P. J., Scheffer, G. L., ter Borg, F., Scheper, R. J., Tytgat, G. N., Borst, P., Baas, F., and Oude Elferink, R. P. (1997) *Hepatology* 25, 1539–42.
29. Wada, M., Toh, S., Taniguchi, K., Nakamura, T., Uchiumi, T., Kohno, K., Yoshida, I., Kimura, A., Sakisaka, S., Adachi, Y., and Kuwano, M. (1998) *Hum. Mol. Genet.* 7, 203–7.
30. Evers, R., Kool, M., van Deemter, L., Janssen, H., Calafat, J., Oomen, L. C., Paulusma, C. C., Oude Elferink, R. P., Baas, F., Schinkel, A. H., and Borst, P. (1998) *J. Clin. Invest.* 101, 1310–9.
31. Cui, Y., Konig, J., Buchholz, J. K., Spring, H., Leier, I., and Keppler, D. (1999) *Mol. Pharmacol.* 55, 929–37.
32. Hirohashi, T., Suzuki, H., and Sugiyama, Y. (1999) *J. Biol. Chem.* 274, 15181–5.
33. Kool, M., van der Linden, M., de Haas, M., Scheffer, G. L., de Vree, J. M., Smith, A. J., Jansen, G., Peters, G. J., Ponne, N., Scheper, R. J., Elferink, R. P., Baas, F., and Borst, P. (1999) *Proc. Natl. Acad. Sci. U.S.A.* 96, 6914–9.
34. Young, L. C., Campling, B. G., Voskoglou-Nomikos, T., Cole, S. P., Deeley, R. G., and Gerlach, J. H. (1999) *Clin. Cancer Res.* 5, 673–80.
35. Bergen, A. A., Plomp, A. S., Schuurman, E. J., Terry, S., Breuning, M., Dauwerse, H., Swart, J., Kool, M., van Soest, S., Baas, F., ten Brink, J. B., and de Jong, P. T. (2000) *Nat. Genet.* 25, 228–31.
36. Le Saux, O., Urban, Z., Tschuch, C., Csiszar, K., Bacchelli, B., Quaglino, D., Pasquali-Ronchetti, I., Pope, F. M., Richards, A., Terry, S., Bercovitch, L., de Paepe, A., and Boyd, C. D. (2000) *Nat. Genet.* 25, 223–7.
37. Daoud, R., Desneves, J., Deady, L. W., Tilley, L., Scheper, R. J., Gros, P., and Georges, E. (2000) *Biochemistry* 39, 6094–102.
38. Daoud, R., Kast, C., Gros, P., and Georges, E. (2000) *Biochemistry* 39, 15344–52.
39. Hipfner, D. R., Mao, Q., Qiu, W., Leslie, E. M., Gao, M., Deeley, R. G., and Cole, S. P. (1999) *J. Biol. Chem.* 274, 15420–6.
40. Taguchi, Y., Yoshida, A., Takada, Y., Komano, T., and Ueda, K. (1997) *FEBS Lett.* 401, 11–4.
41. Chang, X. B., Hou, Y. X., and Riordan, J. R. (1997) *J. Biol. Chem.* 272, 30962–8.
42. Mao, Q., Leslie, E. M., Deeley, R. G., and Cole, S. P. (1999) *Biochim. Biophys. Acta* 1461, 69–82.
43. Gao, M., Cui, H. R., Loe, D. W., Grant, C. E., Almquist, K. C., Cole, S. P., and Deeley, R. G. (2000) *J. Biol. Chem.* 275, 13098–108.
44. Hou, Y., Cui, L., Riordan, J. R., and Chang, X. (2000) *J. Biol. Chem.* 275, 20280–7.
45. Chang, X. B., Hou, Y. X., and Riordan, J. R. (1998) *J. Biol. Chem.* 273, 23844–8.
46. Nagata, K., Nishitani, M., Matsuo, M., Kioka, N., Amachi, T., and Ueda, K. (2000) *J. Biol. Chem.* 275, 17626–30.
47. Ellis, S. B., Brust, P. F., Koutz, P. J., Waters, A. F., Harpold, M. M., and Gingeras, T. R. (1985) *Mol. Cell. Biol.* 5, 1111–21.
48. Tschopp, J. F., Brust, P. F., Cregg, J. M., Stillman, C. A., and Gingeras, T. R. (1987) *Nucleic Acids Res.* 15, 3859–76.
49. Beaudet, L., Urbatsch, I. L., and Gros, P. (1998) *Methods Enzymol.* 292, 397–413.
50. Beaudet, L., Urbatsch, I. L., and Gros, P. (1998) *Biochemistry* 37, 9073–82.
51. Zaman, G. J., Flens, M. J., van Leusden, M. R., de Haas, M., Mulder, H. S., Lankelma, J., Pinedo, H. M., Scheper, R. J., Baas, F., Broxterman, H. J., et al. (1994) *Proc. Natl. Acad. Sci. U.S.A.* 91, 8822–6.
52. Urbatsch, I. L., Beaudet, L., Carrier, I., and Gros, P. (1998) *Biochemistry* 37, 4592–602.
53. Laemmli, U. K. (1970) *Nature* 227, 680–5.
54. Nare, B., Liu, Z., Prichard, R. K., and Georges, E. (1994) *Biochem. Pharmacol.* 48, 2215–22.
55. Georges, E., Zhang, J. T., and Ling, V. (1991) *J. Cell Physiol.* 148, 479–84.
56. Fairbanks, G., Steck, T. L., and Wallach, D. F. (1971) *Biochemistry* 10, 2606–17.
57. Krishnamachary, N., and Center, M. S. (1993) *Cancer Res.* 53, 3658–61.
58. Cole, S. P., Bhardwaj, G., Gerlach, J. H., Mackie, J. E., Grant, C. E., Almquist, K. C., Stewart, A. J., Kurz, E. U., Duncan, A. M., and Deeley, R. G. (1992) *Science* 258, 1650–4.
59. Urbatsch, I. L., Sankaran, B., Weber, J., and Senior, A. E. (1995) *J. Biol. Chem.* 270, 19383–90.
60. Urbatsch, I. L., Gimi, K., Wilke-Mounts, S., and Senior, A. E. (2000) *J. Biol. Chem.* 275, 25031–8.
61. Kwan, T., Loughrey, H., Brault, M., Gruenheid, S., Urbatsch, I. L., Senior, A. E., and Gros, P. (2000) *Mol. Pharmacol.* 58, 37–47.
62. Sonveaux, N., Vigano, C., Shapiro, A. B., Ling, V., and Ruyschaert, J. M. (1999) *J. Biol. Chem.* 274, 17649–54.
63. Loo, T. W., and Clarke, D. M. (1999) *J. Biol. Chem.* 274, 35388–92.
64. Loo, T. W., and Clarke, D. M. (2000) *J. Biol. Chem.* 275, 39272–8.
65. Manciu, L., Chang, X. B., Riordan, J. R., and Ruyschaert, J. M. (2000) *Biochemistry* 39, 13026–33.
66. Le Gal, J. M., Morjani, H., Fardel, O., Guillouzo, A., and Manfait, M. (1994) *Anticancer Res.* 14, 1541–8.
67. Hung, L. W., Wang, I. X., Nikaido, K., Liu, P. Q., Ames, G. F., and Kim, S. H. (1998) *Nature* 396, 703–7.
68. Julien, M., Kajiji, S., Kaback, R. H., and Gros, P. (2000) *Biochemistry* 39, 75–85.

BI010093C